

Nonlinear Dynamical Responses of Composite Laminated Shells with Transverse Excitation

Xiangying Guo^{1,2}, Dameng Liu¹, Wei Zhang^{1,*}

1 Beijing Key Laboratory of Nonlinear Vibrations and Strength of Mechanical Structures, College of Mechanical Engineering, Beijing University of Technology

2 Key Laboratory of Dynamics and Control of Flight Vehicle, Ministry of Education, 100124, P. R. China

Abstract: Please keyin abstract here. The size of the characters is 8 with the abstract bold. An investigation on the nonlinear vibration responses of a composite laminated shell reinforced with carbon nanotubes (CNT) is presented in this paper. The CNT composite laminated shell is simply-supported and doubly curved with rectangular base. The shell is subjected to the parametric excitation along with y direction and transverse excitation. The elasticity modulus of the composite material included the micro and macro materials are calculated by the Mori-Tanaka and the Eshelby's methods. The nonlinear governing partial differential equations of motion for the CNT composite laminated shell are obtained based on the Reddy's third-order shear deformation theory. The 1:1 internal resonance and primary parametric resonance is considered to analyze the nonlinear ordinary differential equations of the shell. Numerical results for dynamic responses and chaotic motions of the CNT composite laminated shell are obtained to investigate the effects of the forcing excitation on the structure.

Keywords: Nonlinear vibrations; carbon nanotubes shell; Mori-Tanaka method

1 Introduction

Carbon nanotubes fillers are worthy of special notice among many different fillers since their positive impact on the polymeric matrix. Nowadays, the CNT reinforced composites are widely used in a variety of engineering applications, especially in aeronautics and astronautics. Therefore, the knowledge of their dynamic behavior are needed to provide more helpful theoretical guidance for the engineering applications.

Nanotubes have extraordinary mechanical, electrical and thermal properties with providing strong, light and high toughness characteristics^[1]. Since Iijima^[2] discovered the carbon nanotubes in 1991, researches related to the nanotubes have been found increasingly for their better mechanical performance^[3-6].

* Corresponding author(sandyzhang0@yahoo.com)

Several investigations on the mechanics of the CNT composite structures can be found in the literatures. A modified rule of mixture has been employed by Tan et al.^[7] to evaluate the elastic properties of such nano composites. Later, the clay was used in the nano layers which are fully dispersed in a polymer matrix to improve the mechanical strength, thermal stability and barrier properties of the material^[8]. At the same time, nanocomposite formation is also reported to improve the performance of the polymer material by incorporation of nanomaterial into the polymer matrix^[9,10]. Zhu et al.^[11] carried out the bending and free vibration analyses of functionally graded carbon nanotube reinforced composite plates.

In recently, using the finite element method (FEM) and the first-order shear deformation theory (FSDT), Shen and Xiang^[12] investigated the large amplitude vibration behaviors of nano composite cylindrical shells reinforced by single-walled carbon nanotubes in thermal environments. Brischetto et al.^[13] analyzed the mechanical behaviors of simply supported nano composite layered cylindrical shell panels. Based on the Halpin-Tsai model to evaluate the dispersing properties of CNT in the matrix, Bhardwaj et al.^[14] studied the nonlinear flexural and dynamic behavior of CNT reinforced laminated composite plates. Moradi-Dastjerdi et al.^[15] investigated the dynamic characters of nano composite cylinders reinforced by single-walled carbon nanotubes with an impact load. Lei et al.^[16] analyzed the dynamic stability of the carbon nanotube-reinforced functionally graded cylindrical panels under the static and periodic axial force by using the mesh-free kpkp-Ritz method. Fazelzadehet et al.^[17] investigated the aeroelastic characteristics of nano composite plates reinforced by carbon nanotubes under the super sonicflow. Phung-Van et al.^[18] studied the static and dynamic behaviors of functionally graded carbon nano-reinforced composite plates by using the isogeometric analysis and higher-order shear deformation theory. Nguyen^[19] presented the nonlinear vibration responses of the imperfect laminated three-phase polymer nanocomposite panel resting on elastic foundations and subjected to hydrodynamic loads. The nano-dynamic mechanical of single-walled carbon nanotubes reinforced nanocomposite thin films were examined via experimental method by Venugopal et al.^[20].

A number of scholars expressed different views and ingenious ideas on the nonlinear dynamic responses of different plates and shells. Amabili^[21] investigated the nonlinear vibrations of doubly curved shallow shells with rectangular base, simply supported at the four edges and subjected to the harmonic excitation normal to the surface in the spectral neighbor hood of the fundamental mode. Eremeyev and Pietraszkiewicz^[22] established the local symmetry group of the dynamic and kinematic theory of elastic shells. Park et al.^[23] discussed the forced vibration responses of skew sandwich plates with laminated faces subjected to various dynamic loads. Besides, some books also introduced the nonlinear dynamics, stability and bifurcation of the composite plates and shells^[24, 25].

Zhang et al.^[26, 27] analyzed the nonlinear vibration responses of composite laminated plates with the transverse and parametric excitations, and analyzed the dynamic behaviors of composite plates related to boundary constraints and load conditions. The nonlinear strain gradient theory of shells was presented by Lazopoulos et al.^[28]. The nonlinear responses of eccentrically stiffened FGM cylindrical panels on elastic

foundation subjected to mechanical loads were presented in article^[29]. Alijani et al.^[30] gave a review on the nonlinear vibrations of different shell structures in the last ten years. Liu et al.^[31] studied the nonlinear vibrations of a simply supported FGM cylindrical shell with small initial geometric imperfection under complex loads. The dynamic independent variables of toroidal shell structures in free space were expressed by Tizzi^[32]. Guo and Zhang^[33] also studied a reinforced composite plate with the carbon nanotubes (CNT) under combined the parametric and forcing excitations.

In this paper, the nonlinear dynamic responses of simply supported symmetric nanotube reinforced composite shell are investigated. The shell is doubly curved with rectangular base and excited by both the in-plane and transverse loads. Based on the Mori-Tanaka method and Reddy's third-order shear deformation theory, the nonlinear governing formulations of motion for the CNT reinforced composite plate are derived. The nonlinear ordinary differential equations are obtained through the two-order Galerkin discretization under the parametric and forcing excitations. Finally, numerical simulation are used to express the periodic and chaotic motions of the CNT-reinforced composite doubly curved shell by the Runge-Kutta algorithm. These results have practical guide significance to the engineering problems in the design of the CNT composite shell structures.

2 Equations of Motion

A mechanical model of a four-edge simply-supported symmetric cross-ply composite shallow shell is considered here as shown in Figure 1. The multi layered fiber shell is reinforced by CNT and doubly curved with rectangular base. (ξ_1, ξ_2, ζ) denote the orthogonal curvilinear coordinates such that ξ_1 and ξ_2 curves are the lines of curvature on the middle surface $\zeta = 0$. The a and b are the curvilinear lengths of the edges and h is the shell thickness. A Cartesian coordinate is located at the middle surface of the shell. The displacements of an arbitrary point within the shell in the coordinates (ξ_1, ξ_2, ζ) are denoted by u , v and w , respectively. The w is taken positive outward from the center of the smallest radius of curvature. The shell is subjected to the in-plane and transverse loads. The in-plane excitation $p = p_0 + p_1 \cos \Omega_2 t$ is along the y direction at $x = a$, and the transverse excitation is assumed to be $F = F_0 + F_1 \cos \Omega_1 t$.

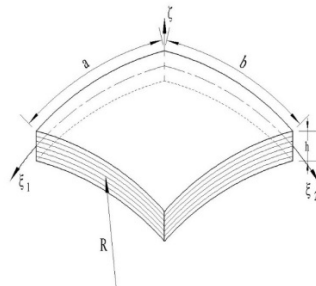


Fig. 1. Composite Doubly Curved Shell Model

The curvilinear coordinates are defined as $s_1 = \alpha_1 R_1$ and $s_2 = \alpha_2 R_2$, where s_1 and s_2 are the lengths, α_1 and α_2 are the angular coordinates and R_1 and R_2 are principal radii of curvature.

There are three assumptions given for the CNT composite laminated shell.

1. The nanotubes with the same shapes are uniformly distributed in the matrix
2. The nanotubes have no agglomeration.
3. Carbon nanotubes are defined as the long hollow cylindrical fibers in the matrix.

The stress-strain relationships for the carbon tubes are given as follows

$$\begin{Bmatrix} \sigma_{11} \\ \sigma_{22} \\ \sigma_{33} \\ \sigma_{23} \\ \sigma_{13} \\ \sigma_{12} \end{Bmatrix} = \begin{bmatrix} k_r + m_r & l_r & k_r - m_r & 0 & 0 & 0 \\ & l_r & n_r & l_r & 0 & 0 \\ k_r - m_r & l_r & k_r + m_r & 0 & 0 & 0 \\ 0 & 0 & 0 & p_r & 0 & 0 \\ 0 & 0 & 0 & 0 & m_r & 0 \\ 0 & 0 & 0 & 0 & 0 & p_r \end{bmatrix} \begin{Bmatrix} \varepsilon_{11} \\ \varepsilon_{22} \\ \varepsilon_{33} \\ 2\varepsilon_{23} \\ 2\varepsilon_{13} \\ 2\varepsilon_{12} \end{Bmatrix} \quad (1)$$

where k_r, l_r, m_r, n_r and p_r are Hill coefficients, specifically, k_r is the bulk modulus for the nanotubes, n_r is the axial tensile modulus, l_r is the transverse modulus, m_r and p_r are shear modulus in the perpendicular and are parallel to the surface of the nanotube direction, respectively^[34].

Then, according to the Mori-Tanaka method^[35], the average stress and strain of the material with two different components can be written as follows

$$\begin{aligned} \sigma_m &= \mathbf{C}_m \varepsilon_m, \quad \sigma_r = \mathbf{C}_r \varepsilon_r, \\ \bar{\sigma} &= \mathbf{c}_m \sigma_m + \mathbf{c}_r \sigma_r, \quad \bar{\varepsilon} = \mathbf{c}_m \varepsilon_m + \mathbf{c}_r \varepsilon_r. \end{aligned} \quad (2)$$

where subscript m and r are short for matrix and reinforced material, and \mathbf{C} means stiffness tensors for the matrix and the reinforced material, respectively.

Then, the CNT are assumed in the large and uniform perfect matrix. Based on the calculating method of the effective module given in Mori-Tanaka theory and the Eshelby's method, the average strain in the fiber material can be calculated to the average composite strain by a strain concentration tensor \mathbf{A} and expressed as follows

$$\varepsilon_r = \mathbf{A} \varepsilon_m, \quad (3)$$

where \mathbf{A} is given as

$$\mathbf{A} = [\mathbf{I} + \mathbf{E} \mathbf{S}_m (\mathbf{C}_r - \mathbf{C}_m)]^{-1}. \quad (4)$$

The concrete expressions of the elastic modulus are shown below when the matrix material is considered as isotropy material

$$\begin{aligned} C_{11} = C_{33} &= \frac{E_m \{E_m c_m + 2k_1(1 + \nu_m)[1 + c_r(1 - 2\nu_m)]\}}{2(1 + \nu_m)E_m(1 + c_r - 2\nu_m) + 2c_m k_r(1 - \nu_m - 2\nu_m^2)} + C_{55}, \\ C_{12} = C_{21} = C_{32} = C_{23} &= \frac{E_m \{c_m \nu_m [E_m + 2k_1(1 + \nu_m)] 2c_r l_r (1 - \nu_m^2)\}}{(1 + \nu_m)[2c_m k_r(1 - \nu_m - 2\nu_m^2) + E_m(1 + c_r - 2\nu_m)]}, \\ C_{13} = C_{31} &= \frac{E_m \{E_m c_m + 2k_1(1 + \nu_m)[1 + c_r(1 - 2\nu_m)]\}}{2(1 + \nu_m)[E_m(1 + c_r - 2\nu_m) + 2c_m k_r(1 - \nu_m - 2\nu_m^2)]} - C_{55}, \end{aligned}$$

$$\begin{aligned}
 C_{22} &= \frac{E_m^2 c_m (1 + c_r - c_m v_m) + 2c_m c_r (k_r n_r - l_r^2) (1 + v_m)^2 (1 - 2v_m)}{(1 + v_m) \{2c_m k_r (1 - v_m - 2v_m^2) + E_m (1 + c_r - 2v_m)\}} \\
 &\quad + \frac{E_m [2c_m^2 k_r (1 - v_m) + c_r n_r (1 - 2v_m + c_r) + 4c_m c_r l_r v_m]}{2c_m k_r (1 - v_m - 2v_m^2) + E_m (1 + c_r - 2v_m)}, \\
 C_{44} &= \frac{E_m [E_m c_m + 2(1 + c_r) p_r (1 + v_m)]}{2(1 + v_m) [E_m (1 + c_r) + 2c_m p_r (1 + v_m)]}, \\
 C_{55} &= \frac{E_m [E_m c_m + 2m(1 + v_m)(3 + c_r - 4v_m)]}{2(1 + v_m) [E_m [c_m - 4c_r(-1 + v_m) - 2c_m m(-3 + v_m + 4v_m^2)]]}. \tag{5}
 \end{aligned}$$

Then, the elasticity modules of axial and transverse for the CNT reinforced composite material are expressed as

$$\bar{E}_{11} = \frac{4C_{55}(C_{11}C_{22} - C_{11}C_{55} - C_{12}^2)}{C_{11}C_{22} - C_{11}C_{55} - C_{12}^2 + C_{22}C_{55}}, \quad \bar{E}_{22} = C_{22} = \frac{C_{12}^2}{C_{11} - C_{55}}. \tag{6}$$

The elastic modulus \bar{Q}_{ij} ($i = 1, 2, 4, 5, 6; j = 1, 2, 4, 5, 6$) of the CNT reinforced composite shell can be expressed as follows

$$\begin{aligned}
 \bar{Q}_{11} &= \frac{\bar{E}_{11}}{1 - \bar{v}_{12}\bar{v}_{21}}, \quad \bar{Q}_{22} = \frac{\bar{E}_{22}}{1 - \bar{v}_{12}\bar{v}_{21}}, \quad \bar{Q}_{12} = \frac{\bar{v}_{12}\bar{E}_{11}}{1 - \bar{v}_{12}\bar{v}_{21}}, \\
 \bar{Q}_{21} &= \frac{\bar{v}_{21}\bar{E}_{22}}{1 - \bar{v}_{12}\bar{v}_{21}}, \quad \bar{Q}_{44} = \bar{G}_{23}, \quad \bar{Q}_{55} = \bar{G}_{13}, \quad \bar{Q}_{66} = \bar{G}_{12}, \tag{7}
 \end{aligned}$$

where the sup bar means equivalent.

The stiffness elements of the symmetric cross-ply composite laminated shell denoted in terms of the stiffness coefficients $(\bar{Q}_{ij})_k$ of the k th layer are

$$(A_{ij}, B_{ij}, D_{ij}, E_{ij}, F_{ij}, H_{ij}) = \sum_{k=1}^n \int_{z_{k-1}}^{z_k} (\bar{Q}_{ij})_k (1, z, z^2, z^3, z^4, z^6) dz. \tag{8}$$

It is found that there exist the following relations

$$A_{16} = A_{26} = D_{16} = D_{26} = F_{16} = F_{26} = H_{16} = H_{26} = 0 \quad \text{and} \quad B_{ij} = E_{ij} = 0. \tag{9}$$

It is seen from equation (9) that there is no coupling between the in-plane stretching and transverse bending. Then, the force and moment resultants related to the strains and curvatures of the shell constitutive equations are expressed in the following form

$$\begin{Bmatrix} N_x \\ N_y \\ N_{xy} \end{Bmatrix} = \begin{Bmatrix} A_{11} & A_{12} & 0 \\ A_{21} & A_{22} & 0 \\ 0 & 0 & A_{66} \end{Bmatrix} \begin{Bmatrix} \epsilon_x^{(0)} \\ \epsilon_y^{(0)} \\ \gamma_{xy}^{(0)} \end{Bmatrix}, \tag{10a}$$

$$\begin{Bmatrix} M_x \\ M_y \\ M_{xy} \end{Bmatrix} = \begin{Bmatrix} D_{11} & D_{12} & 0 \\ D_{21} & D_{22} & 0 \\ 0 & 0 & D_{66} \end{Bmatrix} \begin{Bmatrix} \epsilon_x^{(1)} \\ \epsilon_y^{(1)} \\ \gamma_{xy}^{(1)} \end{Bmatrix} + \begin{Bmatrix} F_{11} & F_{12} & 0 \\ F_{21} & F_{22} & 0 \\ 0 & 0 & F_{66} \end{Bmatrix} \begin{Bmatrix} \epsilon_x^{(2)} \\ \epsilon_y^{(2)} \\ \gamma_{xy}^{(2)} \end{Bmatrix}, \tag{10b}$$

$$\begin{Bmatrix} P_x \\ P_y \\ P_{xy} \end{Bmatrix} = \begin{Bmatrix} F_{11} & F_{12} & 0 \\ F_{21} & F_{22} & 0 \\ 0 & 0 & F_{66} \end{Bmatrix} \begin{Bmatrix} \varepsilon_x^{(1)} \\ \varepsilon_y^{(1)} \\ \gamma_{xy}^{(1)} \end{Bmatrix} + \begin{Bmatrix} H_{11} & H_{12} & 0 \\ H_{21} & H_{22} & 0 \\ 0 & 0 & H_{66} \end{Bmatrix} \begin{Bmatrix} \varepsilon_x^{(2)} \\ \varepsilon_y^{(2)} \\ \gamma_{xy}^{(2)} \end{Bmatrix}, \quad (10c)$$

$$\begin{Bmatrix} Q_y \\ Q_x \end{Bmatrix} = \begin{Bmatrix} A_{44} & 0 \\ 0 & A_{55} \end{Bmatrix} \begin{Bmatrix} \gamma_{yz}^{(0)} \\ \gamma_{xz}^{(0)} \end{Bmatrix}, \quad (10d)$$

$$\begin{Bmatrix} R_y \\ R_x \end{Bmatrix} = \begin{Bmatrix} D_{44} & 0 \\ 0 & D_{55} \end{Bmatrix} \begin{Bmatrix} \gamma_{yz}^{(0)} \\ \gamma_{xz}^{(0)} \end{Bmatrix} + \begin{Bmatrix} F_{44} & 0 \\ 0 & F_{55} \end{Bmatrix} \begin{Bmatrix} \gamma_{yz}^{(2)} \\ \gamma_{xz}^{(2)} \end{Bmatrix}. \quad (10e)$$

Based on the Reddy's third-order shear deformation shell theory, the displacement fields in the CNT reinforced composite shell are expressed as

$$u = u_0 + \zeta\phi_1 - \zeta^3 \frac{4}{3h^2} \left(\phi_1 + \frac{\partial w_0}{\partial x} \right), \quad (11a)$$

$$v = v_0 + \zeta\phi_2 - \zeta^3 \frac{4}{3h^2} \left(\phi_2 + \frac{\partial w_0}{\partial y} \right), \quad (11b)$$

$$w = w_0. \quad (11c)$$

where u_0 , v_0 and w_0 are the original displacements at the mid-plane of the shell in the ξ_1 , ξ_2 and ζ directions, ϕ_1 and ϕ_2 represent the rotations of transverse normal at the mid-plane about the ξ_1 and ξ_2 axes.

Since the thickness of double curvature shallow shells are smaller than the radius of curvature in two directions, we have such expressions as $\left(1 + \frac{\zeta}{R_1}\right) \approx 1$, $\left(1 + \frac{\zeta}{R_2}\right) \approx 1$, where the ζ denotes the displacement of any point on the normal direction of the composite shell. There exist the following conversion relations between curvilinear coordinate system and Cartesian coordinate: $dx = \alpha_1 d\xi_1$, $dy = \alpha_2 d\xi_2$, $dz = d\zeta$, and here α is the surface metric tensor of the composite shell.

The Lamé coefficients of the composite shell are given

$$A_1 = \alpha_1 \left(1 + \frac{\zeta}{R_1}\right), \quad A_2 = \alpha_2 \left(1 + \frac{\zeta}{R_2}\right), \quad A_3 = 1. \quad (12)$$

The shell satisfies the relationship as $dR = A_1 d\xi_1 + A_2 d\xi_2 + \hat{n} d\zeta$, here the \hat{n} is a unit vector normal to the middle surface and denotes as $\hat{n} = \frac{g_1 \times g_2}{a_1 a_2}$. g_1 and g_2 are tangents to the ξ_1 , ξ_2 coordinate lines.

An arbitrary infinitesimal area on the surface of neutral plane of the shell is expressed as

$$dA_\zeta = dR_1 \times dR_2 \cdot \hat{n} = \left(\frac{\partial R}{\partial \xi_1} \times \frac{\partial R}{\partial \xi_2} \cdot \hat{n} \right) d\xi_1 d\xi_2 = A_1 A_2 d\xi_1 d\xi_2. \quad (13)$$

Then, an arbitrary infinitesimal volume on the same plane denotes as

$$dV = dR_1 \times dR_2 \cdot \hat{n} d\zeta = dA_\zeta d\zeta = A_1 A_2 d\xi_1 d\xi_2 d\zeta. \quad (14)$$

According to the Modified Sanders theory, the strains ε_i ($i = xx, yy$) and the curvatures γ_i ($i = xy, yz, zx$) in the mid-plane of the shell can be expressed as

$$\varepsilon_i = \varepsilon_i^0 + \zeta(\varepsilon_i^1 + \zeta^2 \varepsilon_i^2) \quad (i = 1, 2, 6), \quad \varepsilon_i = \varepsilon_i^0 + \zeta^2 \varepsilon_i^1 \quad (i = 4, 5). \quad (15)$$

Here, the specific expressions for the above equation are

$$\begin{aligned} \varepsilon_1^0 &= \frac{\partial u_0}{\partial x} + \frac{w_0}{R_1} + \frac{1}{2} \left(\frac{\partial w_0}{\partial x} \right)^2, \quad \varepsilon_1^2 = -\frac{4}{3h^2} \left(\frac{\partial \varphi_1}{\partial x} + \frac{\partial^2 w_0}{\partial x^2} - \frac{1}{R_1} \frac{\partial u_0}{\partial x} \right) \\ \varepsilon_2^0 &= \frac{\partial v_0}{\partial y} + \frac{w_0}{R_2} + \frac{1}{2} \left(\frac{\partial w_0}{\partial y} \right)^2, \quad \varepsilon_2^2 = -\frac{4}{3h^2} \left(\frac{\partial \varphi_2}{\partial y} + \frac{\partial^2 w_0}{\partial y^2} - \frac{1}{R_2} \frac{\partial v_0}{\partial y} \right) \\ \varepsilon_6^0 &= \frac{\partial v_0}{\partial x} + \frac{\partial u_0}{\partial y} + \frac{\partial w_0}{\partial x} \frac{\partial w_0}{\partial y}, \quad \varepsilon_6^2 = -\frac{4}{3h^2} \left(\frac{\partial \varphi_2}{\partial x} + \frac{\partial \varphi_1}{\partial y} + 2 \frac{\partial^2 w_0}{\partial x \partial y} - \frac{1}{R_2} \frac{\partial v_0}{\partial x} - \frac{1}{R_1} \frac{\partial u_0}{\partial y} \right) \\ \varepsilon_1^1 &= \frac{\partial \phi_1}{\partial x}, \quad \varepsilon_4^0 = \phi_2 + \frac{\partial w_0}{\partial y} - \frac{v_0}{R_2}, \quad \varepsilon_4^1 = -\frac{4}{3h^2} \left(\phi_2 + \frac{\partial w_0}{\partial y} - \frac{v_0}{R_2} \right) \\ \varepsilon_2^1 &= \frac{\partial \phi_2}{\partial y}, \quad \varepsilon_5^0 = \phi_1 + \frac{\partial w_0}{\partial x} - \frac{u_0}{R_1}, \quad \varepsilon_5^1 = -\frac{4}{3h^2} \left(\phi_1 + \frac{\partial w_0}{\partial x} - \frac{u_0}{R_1} \right), \quad \varepsilon_6^1 = \frac{\partial \phi_2}{\partial x} + \frac{\partial \phi_1}{\partial y}. \end{aligned} \quad (16)$$

The force and moment resultants related to the strains and curvatures of the shell constitutive equations then become

$$\begin{Bmatrix} N_x \\ N_y \\ N_{xy} \end{Bmatrix} = \begin{Bmatrix} A_{11} & A_{12} & A_{16} \\ A_{12} & A_{22} & A_{26} \\ A_{16} & A_{26} & A_{66} \end{Bmatrix} \begin{Bmatrix} \varepsilon_x^{(0)} \\ \varepsilon_y^{(0)} \\ \gamma_{xy}^{(0)} \end{Bmatrix}, \quad (17a)$$

$$\begin{Bmatrix} M_x \\ M_y \\ M_{xy} \end{Bmatrix} = \begin{Bmatrix} D_{11} & D_{12} & D_{16} \\ D_{12} & D_{22} & D_{26} \\ D_{16} & D_{26} & D_{66} \end{Bmatrix} \begin{Bmatrix} \kappa_x^{(0)} \\ \kappa_y^{(0)} \\ \kappa_{xy}^{(0)} \end{Bmatrix} + \begin{Bmatrix} F_{11} & F_{12} & F_{16} \\ F_{12} & F_{22} & F_{26} \\ F_{16} & F_{26} & F_{66} \end{Bmatrix} \begin{Bmatrix} \kappa_x^{(2)} \\ \kappa_y^{(2)} \\ \kappa_{xy}^{(2)} \end{Bmatrix}, \quad (17b)$$

$$\begin{Bmatrix} P_x \\ P_y \\ P_{xy} \end{Bmatrix} = \begin{Bmatrix} F_{11} & F_{12} & F_{16} \\ F_{12} & F_{22} & F_{26} \\ F_{16} & F_{26} & F_{66} \end{Bmatrix} \begin{Bmatrix} \kappa_x^{(0)} \\ \kappa_y^{(0)} \\ \kappa_{xy}^{(0)} \end{Bmatrix} + \begin{Bmatrix} H_{11} & H_{12} & H_{16} \\ H_{21} & H_{22} & H_{26} \\ H_{16} & H_{26} & H_{66} \end{Bmatrix} \begin{Bmatrix} \kappa_x^{(2)} \\ \kappa_y^{(2)} \\ \kappa_{xy}^{(2)} \end{Bmatrix}, \quad (17c)$$

$$\begin{Bmatrix} Q_y \\ Q_x \end{Bmatrix} = \begin{Bmatrix} A_{44} & A_{45} \\ A_{45} & A_{55} \end{Bmatrix} \begin{Bmatrix} \gamma_{yz}^{(0)} \\ \gamma_{xz}^{(0)} \end{Bmatrix}, \quad (17d)$$

$$\begin{Bmatrix} R_y \\ R_x \end{Bmatrix} = \begin{Bmatrix} D_{44} & D_{45} \\ D_{45} & D_{55} \end{Bmatrix} \begin{Bmatrix} \gamma_{yz}^{(0)} \\ \gamma_{xz}^{(0)} \end{Bmatrix} + \begin{Bmatrix} F_{44} & F_{45} \\ F_{54} & F_{55} \end{Bmatrix} \begin{Bmatrix} \gamma_{yz}^{(2)} \\ \gamma_{xz}^{(2)} \end{Bmatrix}. \quad (17e)$$

The nonlinear governing equations of motion for the CNT composite laminated shell can be derived by using Hamilton's principle in terms of generalized displacements as follows

$$\begin{aligned}
 & \left(A_{12} + A_{66} + \frac{c_1^2}{R_1 R_2} H_{12} + \frac{c_1^2}{R_1 R_2} H_{66} \right) \frac{\partial^2 v_0}{\partial x \partial y} - \frac{c_1^2}{R_1} H_{11} \frac{\partial^3 w_0}{\partial x^3} + \frac{c_1}{R_1} F_{66} \frac{\partial^2 \phi_2}{\partial y^2} + \frac{c_1}{R_1} F_{66} \frac{\partial^2 \phi_1}{\partial x \partial y} \\
 & + (A_{11} + A_{12}) \frac{\partial w_0}{\partial x} \frac{\partial^2 w_0}{\partial x^2} + \left(A_{11} - \frac{c_1^2}{R_1^2} H_{11} \right) \frac{\partial^2 u_0}{\partial x^2} + A_{66} \frac{\partial^2 w_0}{\partial x \partial y} \frac{\partial w_0}{\partial y} + \left(A_{66} + \frac{c_1^2}{R_1^2} H_{66} \right) \frac{\partial^2 u_0}{\partial y^2} \\
 & + A_{66} \frac{\partial w_0}{\partial x} \frac{\partial^2 w_0}{\partial y^2} + \left(\frac{c_1}{R_1} F_{12} - \frac{c_1^2}{R_1} H_{12} - \frac{c_1^2}{R_1} H_{66} \right) \frac{\partial^2 \phi_2}{\partial x \partial y} + \left(\frac{c_1}{R_1} F_{11} - \frac{c_1^2}{R_1} H_{11} \right) \frac{\partial^2 \phi_1}{\partial x^2} \\
 & + \left(-\frac{c_1^2}{R_1} H_{12} - \frac{2c_1^2}{R_1} H_{66} \right) \frac{\partial^3 w_0}{\partial^2 y \partial x} + \left(\frac{1}{R_1} A_{11} + \frac{1}{R_2} A_{12} + \frac{1}{R_1} A_{55} - \frac{2c_2}{R_1} D_{55} + \frac{c_2^2}{R_1} F_{55} \right) \frac{\partial w_0}{\partial x} \\
 & - \frac{c_1^2}{R_1} H_{66} \frac{\partial^2 \phi_1}{\partial y^2} + \left(\frac{1}{R_1} A_{55} - \frac{2c_2}{R_1} D_{55} + \frac{c_2^2}{R_1} F_{55} \right) \phi_1 \\
 & + \left(-\frac{1}{R_1^2} A_{55} + \frac{2c_2}{R_1^2} D_{55} - \frac{c_2^2}{R_1^2} F_{55} \right) u_0 = I_0 \ddot{u}_0, \tag{18a}
 \end{aligned}$$

$$\begin{aligned}
 & \left(A_{21} + A_{66} + \frac{c_1^2}{R_1 R_2} H_{21} + \frac{c_1^2}{R_1 R_2} H_{66} \right) \frac{\partial^2 u_0}{\partial x \partial y} - \frac{c_1^2}{R_2} H_{22} \frac{\partial^3 w_0}{\partial y^3} + \frac{c_1}{R_2} F_{66} \frac{\partial^2 \phi_1}{\partial x^2} + \frac{c_1}{R_2} F_{66} \frac{\partial^2 \phi_2}{\partial x \partial y} \\
 & + (A_{22} + A_{12}) \frac{\partial w_0}{\partial x} \frac{\partial^2 w_0}{\partial x^2} + \left(A_{22} - \frac{c_1^2}{R_2^2} H_{22} \right) \frac{\partial^2 v_0}{\partial y^2} + A_{66} \frac{\partial w_0}{\partial x} \frac{\partial^2 w_0}{\partial x \partial y} + \left(A_{66} + \frac{c_1^2}{R_2^2} H_{66} \right) \frac{\partial^2 v_0}{\partial x^2} \\
 & + A_{66} \frac{\partial^2 w_0}{\partial x^2} \frac{\partial w_0}{\partial y} + \left(\frac{c_1}{R_2} F_{21} - \frac{c_1^2}{R_2} H_{21} - \frac{c_1^2}{R_2} H_{66} \right) \frac{\partial^2 \phi_1}{\partial x \partial y} + \left(\frac{c_1}{R_2} F_{22} - \frac{c_1^2}{R_2} H_{22} \right) \frac{\partial^2 \phi_2}{\partial y^2} \\
 & + \left(-\frac{c_1^2}{R_2} H_{21} - \frac{2c_1^2}{R_2} H_{66} \right) \frac{\partial^3 w_0}{\partial y \partial x^2} + \left(\frac{1}{R_1} A_{21} + \frac{1}{R_2} A_{22} + \frac{1}{R_2} A_{44} - \frac{2c_2}{R_2} D_{44} + \frac{c_2^2}{R_2} F_{44} \right) \frac{\partial w_0}{\partial y} \\
 & - \frac{c_1^2}{R_2} H_{66} \frac{\partial^2 \phi_2}{\partial x^2} + \left(\frac{1}{R_2} A_{44} - \frac{2c_2}{R_2} D_{44} + \frac{c_2^2}{R_2} F_{44} \right) \phi_2 \\
 & + \left(-\frac{1}{R_2^2} A_{44} + \frac{2c_2}{R_2^2} D_{44} - \frac{c_2^2}{R_2^2} F_{44} \right) v_0 = I_0 \ddot{v}_0, \tag{18}
 \end{aligned}$$

b)

$$\begin{aligned}
 & (A_{55} - 2c_2 D_{55} + c_2^2 F_{55}) \frac{\partial \phi_1}{\partial x} + \left(-\frac{1}{R_1} A_{55} + \frac{2}{R_1} c_2 D_{55} - \frac{1}{R_1} c_2^2 F_{55} - \frac{1}{R_1} A_{11} - \frac{1}{R_2} A_{21} \right) \frac{\partial u_0}{\partial x} \\
 & + (A_{44} - 2c_2 D_{44} + c_2^2 F_{44}) \frac{\partial \phi_2}{\partial y} + \left(-\frac{1}{R_2} A_{44} + \frac{2}{R_2} c_2 D_{44} - \frac{c_2^2 F_{44}}{R_2} - \frac{A_{12}}{R_1} - \frac{A_{22}}{R_2} \right) \frac{\partial v_0}{\partial y} \\
 & + (A_{55} - 2c_2 D_{55} + c_2^2 F_{55} - N_1^p + p_x) \frac{\partial^2 w_0}{\partial x^2} + (A_{44} - 2c_2 D_{44} + c_2^2 F_{44} - N_2^p + p_y) \frac{\partial^2 w_0}{\partial y^2} \\
 & + \left(-\frac{A_{11}}{R_1^2} - \frac{A_{12}}{R_1 R_2} - \frac{A_{21}}{R_1 R_2} - \frac{A_{22}}{R_2^2} \right) w_0 + \left(-\frac{1}{R_1} A_{11} - \frac{1}{2R_2} A_{21} + \frac{1}{R_2} A_{12} \right) \left(\frac{\partial w_0}{\partial x} \right)^2
 \end{aligned}$$

$$\begin{aligned}
 & + \left(-\frac{1}{R_2} A_{22} - \frac{1}{2R_1} A_{12} + \frac{1}{R_1} A_{21} \right) \left(\frac{\partial w_0}{\partial y} \right)^2 + (c_1 F_{11} - c_1^2 H_{11}) \frac{\partial^3 \phi_1}{\partial x^3} + (-c_1^2 H_{11}) \frac{\partial^4 w_0}{\partial x^4} \\
 & + \frac{c_1^2 H_{11}}{R_1} \frac{\partial^3 w_0}{\partial x^3} + (c_1 F_{12} - c_1^2 H_{12} - 2c_1^2 H_{66}) \frac{\partial^3 \phi_2}{\partial x^2 \partial y} + \left(\frac{1}{R_2} c_1^2 H_{12} + \frac{2}{R_2} c_1^2 H_{66} \right) \frac{\partial^3 v_0}{\partial x^2 \partial y} \\
 & + (-c_1^2 H_{12} - c_1^2 H_{21} - c_1^2 H_{22} - 4c_1^2 H_{66}) \frac{\partial^4 w_0}{\partial x^2 \partial y^2} + (c_1 F_{21} - 2c_1^2 H_{66} - c_1^2 H_{21}) \frac{\partial^3 \phi_1}{\partial x \partial y^2} \\
 & + (c_1 F_{22} - c_1^2 H_{22}) \frac{\partial^3 \phi_2}{\partial y^3} + \left(\frac{1}{R_1} c_1^2 H_{21} \right) \frac{\partial^3 u_0}{\partial y \partial x^2} + \left(\frac{1}{R_2} c_1^2 H_{22} \right) \frac{\partial^3 v_0}{\partial y^3} + (2c_1 F_{66}) \frac{\partial^3 \phi_1}{\partial y \partial x^2} \\
 & + (2c_1 F_{66}) \frac{\partial^3 \phi_2}{\partial y^2 \partial x} + \left(\frac{2}{R_1} c_1^2 H_{66} \right) \frac{\partial^3 u_0}{\partial y^2 \partial x} + A_{11} \frac{\partial w_0}{\partial x} \frac{\partial^2 u_0}{\partial x^2} + \frac{3}{2} A_{11} \frac{\partial^2 w_0}{\partial x^2} \left(\frac{\partial w_0}{\partial x} \right)^2 \\
 & + (A_{12} + A_{66}) \frac{\partial w_0}{\partial x} \frac{\partial^2 v_0}{\partial x \partial y} + (A_{12} + 4A_{66} + A_{21}) \frac{\partial w_0}{\partial x} \frac{\partial w_0}{\partial y} \frac{\partial^2 w_0}{\partial x \partial y} + A_{12} \frac{\partial^2 w_0}{\partial x^2} \frac{\partial v_0}{\partial y} \\
 & + \left(\frac{1}{R_1} A_{11} + \frac{1}{R_2} A_{12} \right) \frac{\partial^2 w_0}{\partial x^2} w_0 + \left(\frac{1}{2} A_{12} + A_{66} \right) \frac{\partial^2 w_0}{\partial x^2} \left(\frac{\partial w_0}{\partial y} \right)^2 + (A_{66} + A_{21}) \frac{\partial w_0}{\partial y} \frac{\partial^2 u_0}{\partial x \partial y} \\
 & + A_{66} \frac{\partial w_0}{\partial y} \frac{\partial^2 v_0}{\partial x^2} + 2A_{66} \frac{\partial^2 w_0}{\partial x \partial y} \frac{\partial u_0}{\partial y} + 2A_{66} \frac{\partial^2 w_0}{\partial x \partial y} \frac{\partial v_0}{\partial x} + \left(\frac{1}{2} A_{21} + A_{66} \right) \frac{\partial^2 w_0}{\partial y^2} \left(\frac{\partial w_0}{\partial x} \right)^2 \\
 & + A_{66} \frac{\partial w_0}{\partial x} \frac{\partial^2 u_0}{\partial y^2} + A_{22} \frac{\partial w_0}{\partial y} \frac{\partial^2 v_0}{\partial y^2} + \frac{3}{2} A_{22} \frac{\partial^2 w_0}{\partial y^2} \left(\frac{\partial w_0}{\partial y} \right)^2 + A_{21} \frac{\partial^2 w_0}{\partial y^2} \frac{\partial u_0}{\partial x} + A_{22} \frac{\partial^2 w_0}{\partial y^2} \frac{\partial v_0}{\partial y} \\
 & + A_{11} \frac{\partial^2 w_0}{\partial x^2} \frac{\partial u_0}{\partial x} + \left(\frac{1}{R_1} A_{21} + \frac{1}{R_2} A_{22} \right) \frac{\partial^2 w_0}{\partial y^2} w_0 + F \cos \Omega_1 t - \mu \dot{w}_0 \\
 & = c_1 \left[I_3 \left(\frac{\partial \ddot{u}_0}{\partial x} + \frac{\partial \ddot{v}_0}{\partial y} \right) + I_4 \left(\frac{\partial \ddot{\phi}_1}{\partial x} + \frac{\partial \ddot{\phi}_2}{\partial y} \right) \right] \\
 & - c_1^2 \left[I_6 \left(\frac{\partial \ddot{\phi}_1}{\partial x} + \frac{\partial \ddot{\phi}_2}{\partial y} \right) + I_6 \left(\frac{\partial^2 \ddot{w}_0}{\partial x^2} + \frac{\partial^2 \ddot{w}_0}{\partial y^2} \right) \right] + I_0 \ddot{w}_0, \tag{18c}
 \end{aligned}$$

$$\begin{aligned}
 & (D_{11} - 2c_1 F_{11} + c_1^2 H_{11}) \frac{\partial^2 \phi_1}{\partial x^2} + (D_{12} - 2c_1 F_{12} - c_1 F_{66} + c_1^2 H_{12} + c_1^2 H_{66}) \frac{\partial^2 \phi_2}{\partial x \partial y} \\
 & + \left(\frac{1}{R_1} c_1 F_{11} - \frac{1}{R_1} c_1^2 H_{11} \right) \frac{\partial^2 u_0}{\partial x^2} + (-c_1 F_{12} - 2c_1 F_{66} + c_1^2 H_{12} + 2c_1^2 H_{66}) \frac{\partial^3 w_0}{\partial x \partial y^2} \\
 & + (c_1^2 H_{11} - c_1 F_{11}) \frac{\partial^3 w_0}{\partial x^3} + \left(\frac{1}{R_2} c_1 F_{12} + \frac{1}{R_2} c_1 F_{66} - \frac{1}{R_2} c_1^2 H_{12} - \frac{1}{R_2} c_1^2 H_{66} \right) \frac{\partial^2 v_0}{\partial x \partial y} \\
 & + (D_{66} - c_1 F_{66}) \frac{\partial^2 \phi_2}{\partial y^2} + (D_{66} - c_1 F_{66}) \frac{\partial^2 \phi_1}{\partial x \partial y} + \left(\frac{1}{R_1} c_1 F_{66} - \frac{1}{R_1} c_1^2 H_{66} \right) \frac{\partial^2 u_0}{\partial y^2}
 \end{aligned}$$

$$\begin{aligned}
 & + (-A_{55} + 2c_2D_{55} - c_2^2F_{55})\phi_1 + (c_1^2H_{66} - c_1F_{66})\frac{\partial^2\phi_1}{\partial y^2} + (-A_{55} + 2c_2D_{55} - c_2^2F_{55})\frac{\partial w_0}{\partial x} \\
 & + \left(\frac{1}{R_1}A_{55} - \frac{1}{R_1}2c_2D_{55} + \frac{1}{R_1}c_2^2F_{55} \right) u_0 \\
 & = I_1\ddot{u}_0 + I_2\ddot{\phi}_1 - c_1I_4\ddot{\phi}_1 - c_1I_4\frac{\partial\ddot{w}_0}{\partial x} + c_1\left(-I_3\ddot{u}_0 - I_4\ddot{\phi}_1 + c_1I_6\ddot{\phi}_1 + c_1I_6\frac{\partial\ddot{w}_0}{\partial x} \right), \quad (18d) \\
 & (D_{22} - 2c_1F_{22} + c_1^2H_{22})\frac{\partial^2\phi_2}{\partial y^2} + (D_{21} - 2c_1F_{21} - c_1F_{66} + c_1^2H_{21} + c_1^2H_{66})\frac{\partial^2\phi_1}{\partial x\partial y} \\
 & + \left(\frac{1}{R_2}c_1F_{22} - \frac{1}{R_2}c_1^2H_{22} \right)\frac{\partial^2v_0}{\partial y^2} + (-c_1F_{21} - 2c_1F_{66} + c_1^2H_{21} + 2c_1^2H_{66})\frac{\partial^3w_0}{\partial x^2\partial y} \\
 & + (c_1^2H_{22} - c_1F_{22})\frac{\partial^3w_0}{\partial y^3} + \left(\frac{1}{R_1}c_1F_{21} + \frac{1}{R_1}c_1F_{66} - \frac{1}{R_1}c_1^2H_{21} - \frac{1}{R_1}c_1^2H_{66} \right)\frac{\partial^2u_0}{\partial x\partial y} \\
 & + (D_{66} - c_1F_{66})\frac{\partial^2\phi_1}{\partial x^2} + (D_{66} - c_1F_{66})\frac{\partial^2\phi_2}{\partial x\partial y} + \left(\frac{1}{R_2}c_1F_{66} - \frac{1}{R_2}c_1^2H_{66} \right)\frac{\partial^2v_0}{\partial x^2} \\
 & + (-A_{44} + 2c_2D_{44} - c_2^2F_{44})\phi_2 + (c_1^2H_{66} - c_1F_{66})\frac{\partial^2\phi_2}{\partial x^2} + (-A_{44} + 2c_2D_{44} - c_2^2F_{44})\frac{\partial w_0}{\partial y} \\
 & + \left(\frac{1}{R_2}A_{44} - \frac{1}{R_2}2c_2D_{44} + \frac{1}{R_2}c_2^2F_{44} \right) v_0 \\
 & = I_1\ddot{v}_0 + I_2\ddot{\phi}_2 - c_1I_4\ddot{\phi}_2 - c_1I_4\frac{\partial\ddot{w}_0}{\partial y} + c_1\left(-I_3\ddot{v}_0 - I_4\ddot{\phi}_2 + c_1I_6\ddot{\phi}_2 + c_1I_6\frac{\partial\ddot{w}_0}{\partial y} \right). \quad (18e)
 \end{aligned}$$

where μ in equation (18c) is the damping coefficient.

The associated boundary conditions for the simply-supported CNT composite laminated shell are as follows:

$$x = 0 \text{ and } x = a, \quad v = w = 0, \quad \varphi_y = 0, \quad M_{xx} = N_{xy} = 0, \quad (19a)$$

$$y = 0 \text{ and } y = b, \quad v = w = 0, \quad \varphi_x = 0, \quad M_{yy} = N_{xy} = 0, \quad (19b)$$

$$\int_{\frac{h}{2}}^{\frac{h}{2}} N_{xx} dz = \pm \int_{\frac{h}{2}}^{\frac{h}{2}} f dz, \quad (x = 0, a) \quad (19c)$$

3 Perturbation Analysis

In this paper, we consider the nonlinear dynamical system of the double curved shell in its first two modes of the 1:1 inner resonance. Hence, we express W in the form of

$$w = w_1 \sin \frac{3\pi x}{a} \sin \frac{\pi y}{b} + w_2 \sin \frac{\pi x}{a} \sin \frac{3\pi y}{b}, \quad (20)$$

where w_1 and w_2 are the amplitudes of two modes.

The other variables can be written as

$$u = u_1 \sin \frac{3\pi x}{a} \cos \frac{\pi y}{b} + u_2 \sin \frac{\pi x}{a} \cos \frac{3\pi y}{b}, \quad (21a)$$

$$v = v_1 \cos \frac{3\pi x}{a} \sin \frac{\pi y}{b} + v_2 \cos \frac{\pi x}{a} \sin \frac{3\pi y}{b}, \quad (21b)$$

$$\varphi_x = \varphi_1 \cos \frac{3\pi x}{a} \sin \frac{\pi y}{b} + \varphi_2 \cos \frac{\pi x}{a} \sin \frac{3\pi y}{b}, \quad (21c)$$

$$\varphi_y = \varphi_3 \sin \frac{3\pi x}{a} \cos \frac{\pi y}{b} + \varphi_4 \sin \frac{\pi x}{a} \cos \frac{3\pi y}{b}. \quad (21d)$$

Likewise, the transverse excitation can be represented as

$$F = F_1 \sin \frac{3\pi x}{a} \sin \frac{\pi y}{b} + F_2 \sin \frac{\pi x}{a} \sin \frac{3\pi y}{b}. \quad (22)$$

Then, doing the dimensionless processing for the equations (18) and taking all these resulting expressions into equation (18c), the governing differential equations of transverse motion for the CNT reinforced composite laminated shell are formulated by applying the Galerkin procedure

$$\begin{aligned} \ddot{x}_1 + \mu_1 \dot{x}_1 + \omega_1^2 x_1 + a_1 x_1 \cos \Omega_2 t + a_2 x_1^3 + a_3 x_2^3 + a_4 x_1^2 x_2 \\ + a_5 x_1 x_2^2 + a_6 x_1 x_2 + a_7 x_1^2 + a_8 x_2^2 = f_1 \cos \Omega_1 t, \end{aligned} \quad (23a)$$

$$\begin{aligned} \ddot{x}_2 + \mu_2 \dot{x}_2 + \omega_2^2 x_2 + b_1 x_2 \cos \Omega_2 t + b_2 x_1^3 + b_3 x_2^3 + b_4 x_1^2 x_2 \\ + b_5 x_1 x_2^2 + b_6 x_1 x_2 + b_7 x_1^2 + b_8 x_2^2 = f_2 \cos \Omega_1 t, \end{aligned} \quad (23b)$$

From equations (23), it is obvious that the dynamical system of the CNT composite laminated shell is governed by nonlinear square and cubic terms, parametric and force excitation terms.

4 Numerical Simulation and Discussion

In this section, we present a comparative study to find the complex nonlinear dynamical responses of the CNT composite laminated shell. First, the nonlinear governing control equations (23) of the shell are used to perform the numerical simulation. The parameters and the initial values are chosen in the following form $\mu_1 = 0.9$, $a_1 = 94.5$, $a_2 = 15.8$, $a_3 = 97.3$, $a_4 = 28.0$, $a_5 = 98.3$, $a_6 = 18.4$, $a_7 = 53.4$, $a_8 = -47.0$, $\mu_2 = 0.5$, $b_1 = 97.2$, $b_2 = 37.0$, $b_3 = 38.6$, $b_4 = 78.1$, $b_5 = 53.5$, $b_6 = 15.8$, $b_7 = 94.5$, $b_8 = -21.5$, $x_1 = 0.6$, $x_2 = 0.6$, $x_3 = 0.8$, $x_4 = 1.0$. The frequency-response curves of the first-order and second-order are obtained as shown in Figure 2, where the horizontal axis respects the detuning parameter σ and the vertical axis is the amplitudes of the first and second order modes of the CNT

reinforced composite shell, respectively. It is also shown that the system exhibits the hard spring character when the detuning parameter $\sigma > 0$. The jump phenomenon appears in diagrams (c) and (d) when the nonlinear parameters b_4 is equal to -37.78 . This phenomenon reveals that the system is unstable in this stage and exists the multi value solutions in this area.

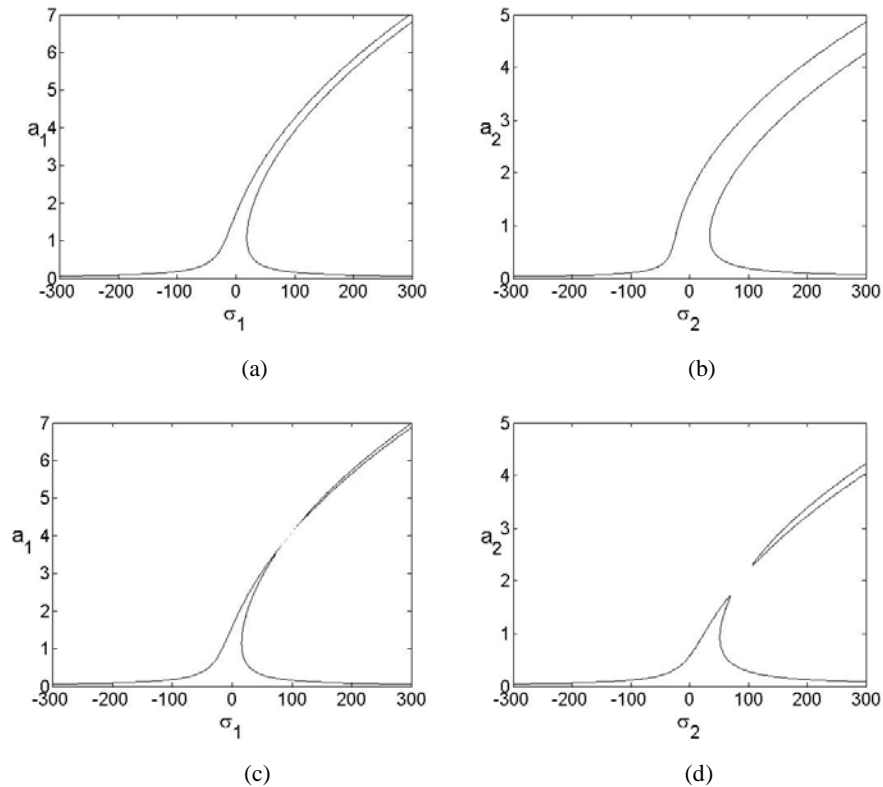


Fig. 2. Response-frequency curves

Then, since transverse excitation also plays an important effect on the nonlinear vibration responses of the structure, the transverse excitation f is chosen to be a controlling parameter in the subsequent studies. Fixed the above parameters and increased the excitation f from 20 to 80, bifurcation diagrams of Poincare sections for the displacement of the shell are obtained as shown in Figure 3. It shows the complex nonlinear dynamics of the system in these parameters. Simple periodic motion, period-doubling bifurcation, sub-harmonic response, amplitude modulations and chaotic motions have been detected. As seen in the figure, the system shows chaotic motions until the transverse excitation f reaching to 38, where period motion occurs. This period-n motion attractor prevails in the range of 38-41, then the chaotic motion is observed again until the transverse excitation f equal to 60. After short windows of period-n motions occurs in 60-68, the motions dominantly enter into chaotic motions

thereafter. The motion characters of the CNT reinforced composite laminated shell alternately appeared from stable to unstable, which depended on the amplitude of the transverse excitation.

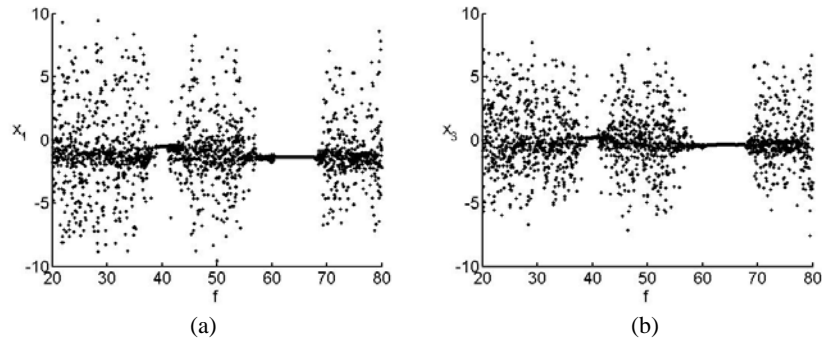
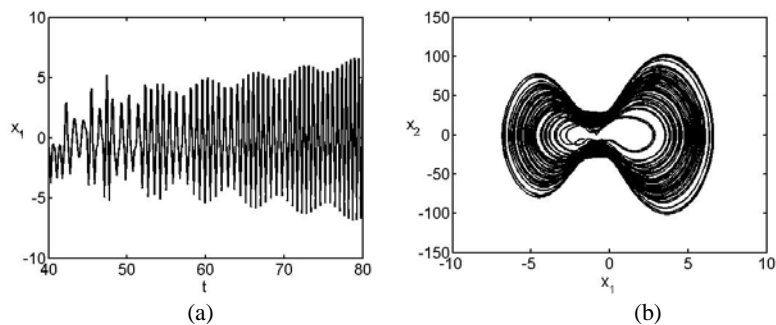


Fig. 3. The bifurcation diagram for increasing amplitude of the transverse excitation variations on the system

To expose the specific form of different sections in the bifurcation diagram, the response-frequency curves, phase portraits, power spectrums and waveforms of the shell are depicted as Figures 4-11. In these figures, diagrams (a) represent the three-dimensional phase portraits in the space (x_1, x_2, x_3) while diagrams (b) represent the power spectrums. Diagrams (c) and (d) are, respectively, the two-dimensional phase portraits on the planes (t, x_1) and the wave forms on the plane (t, x_3) .

In Figures 4-5, we observe that chaotic motions of the CNT composite laminated shell when the transversal excitation $f = 24$ and $f = 29.5$, respectively. By increasing the transversal excitation f to 39.3, we show the periodic-n motion of the shell in the Figure 6. The motion of the shell is back to the periodic-n motion when $f = 46.2$, as displayed in Figure 7. Increasing the transversal excitation f continuously, the system is returned back to the chaotic motion for $f = 53$ as depicted in Figure 8. Then, the periodic-n motion of the system is appearing as shown in Figures 9-10 and when the transversal excitation f are equal to 74, the system is back to the chaotic motion again as shown in Figure 11.



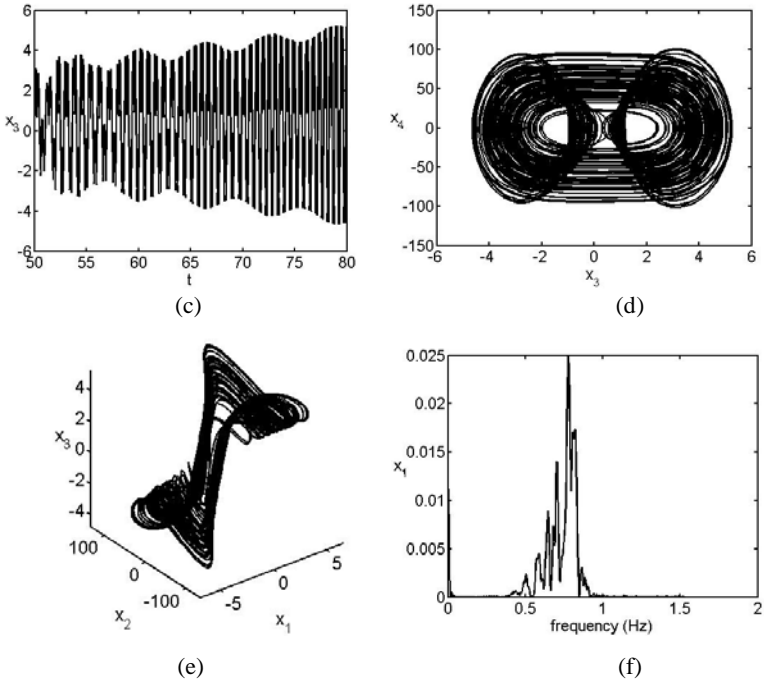
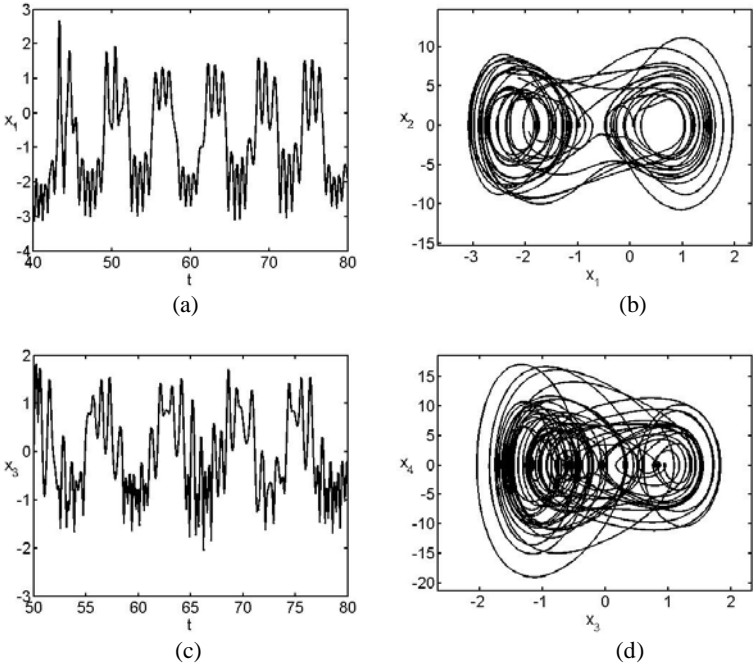


Fig. 4. The chaotic motion of the shell with $f = 24.0$



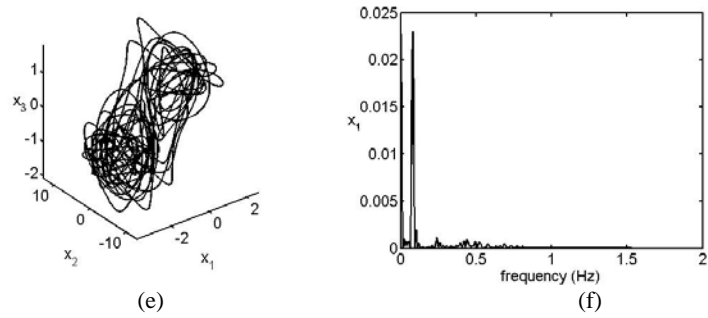


Fig. 5. The chaotic motion of the shell with $f = 29.5$

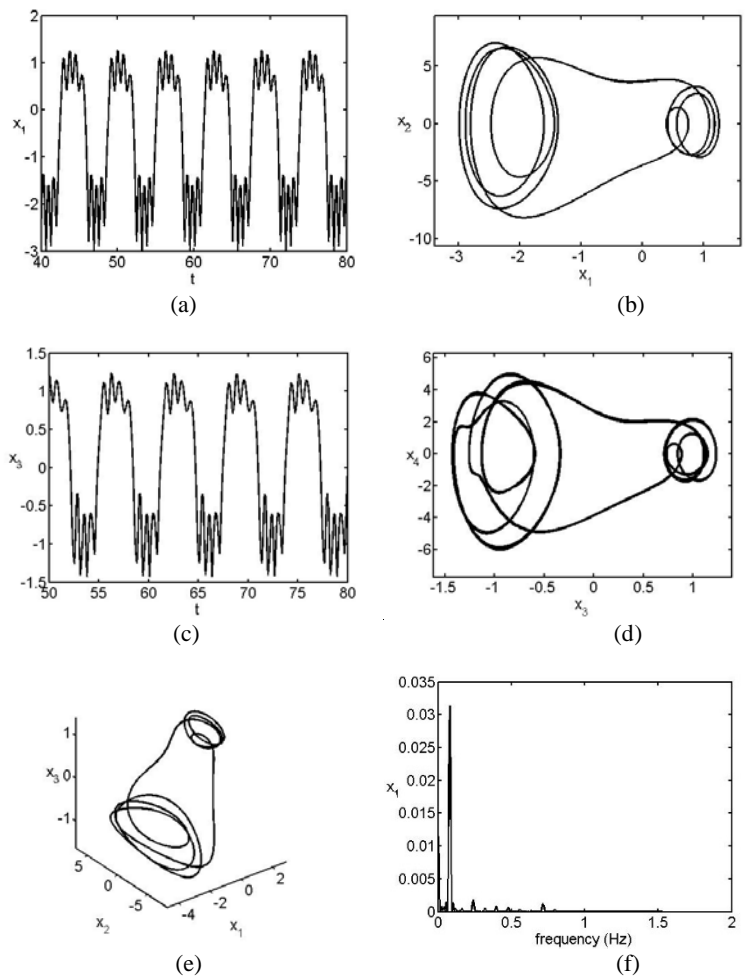


Fig. 6. The periodic-n motion of the shell with $f = 39.3$

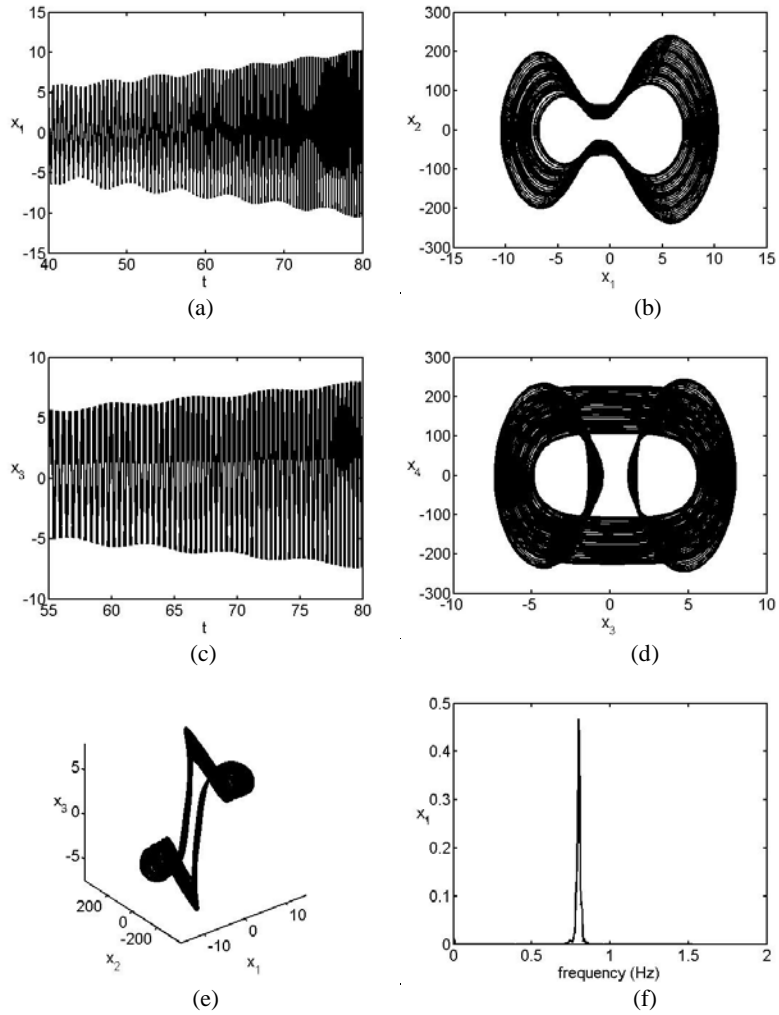
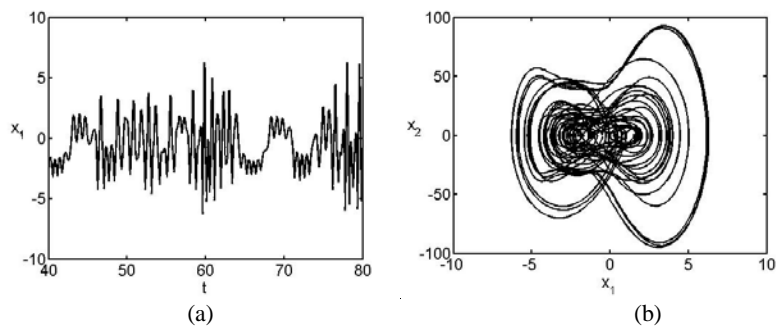


Fig. 7. The periodic-n motion of the shell with $f = 46.2$



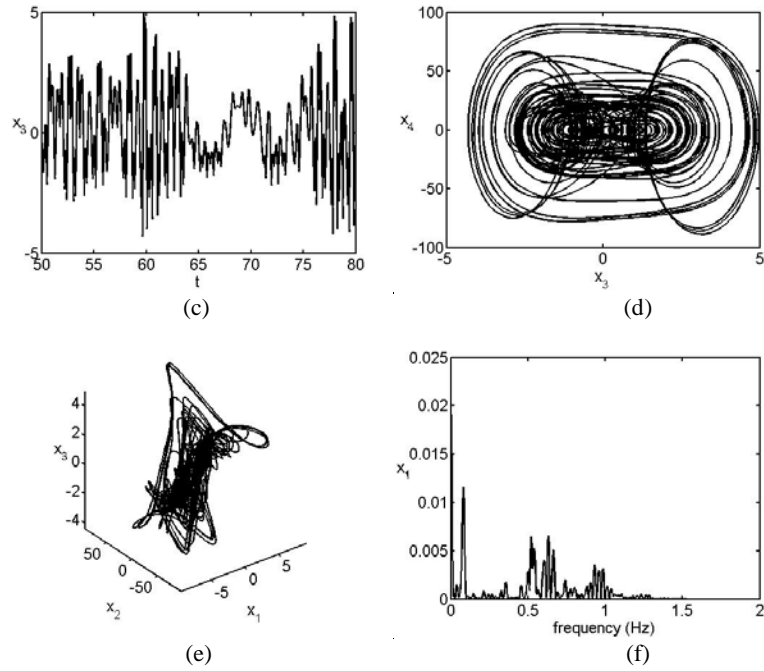
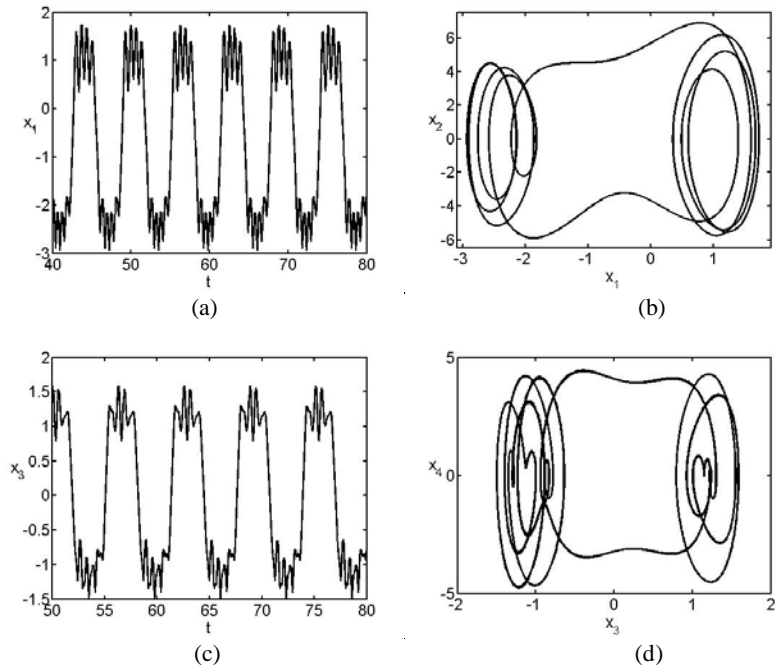


Fig. 8. The chaotic motion of the shell with $f = 53.0$



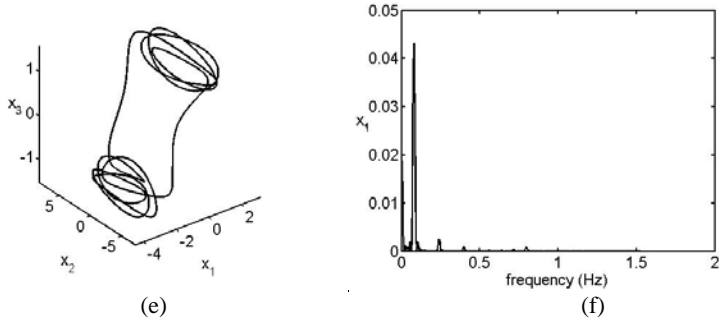


Fig. 9. The periodic-n motion of the shell with $f = 63.0$

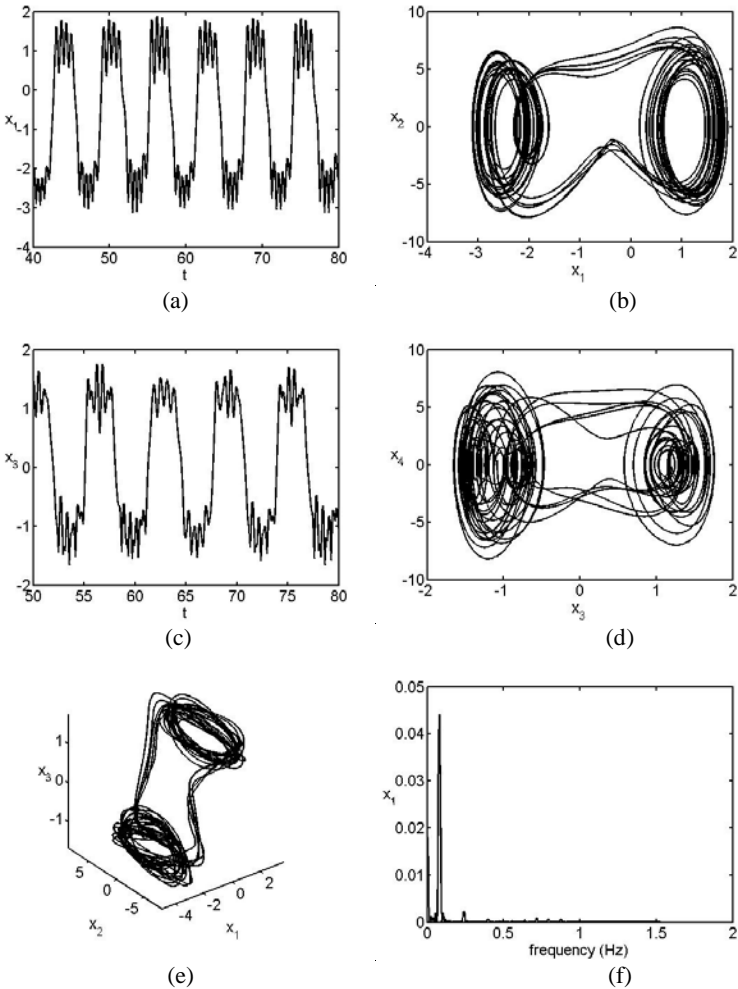


Fig. 10. The periodic-n motion of the shell with $f = 68.2$

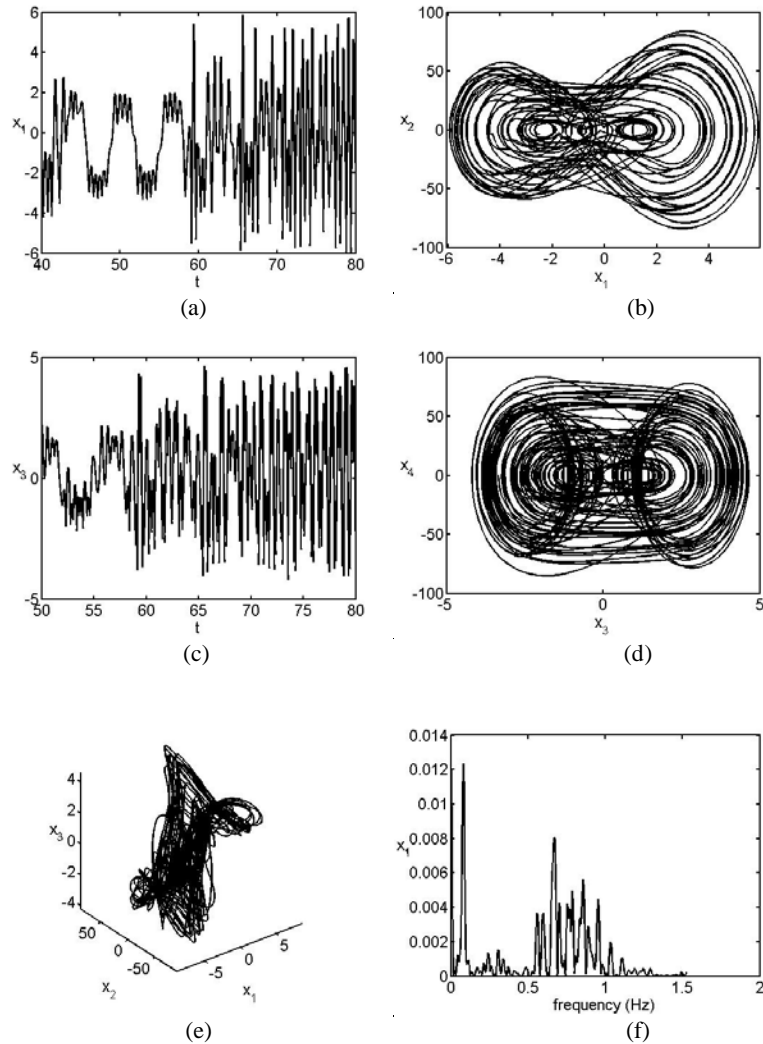


Fig. 11. The chaotic motion of the shell with $f = 74.0$

From the above simulation results of the internal resonance systems, it is found that the nonlinear vibration responses of the CNT composite laminated shell are very complex under the transverse excitations. We can control the motion of the CNT composite laminated shell through adjusting the transversal excitations.

5 Conclusions

Nonlinear dynamics of a CNT reinforced composite double-curved shell are studied in this paper by theoretical analysis and numerical simulation. The shell is excited by

the in-plane and transverse loads. Firstly, the average strain and stress in the reinforced material can be obtained by using the Mori-Tanaka theory and the Eshelby's method. Then, governing partial differential equations of motion for the CNT composite shell are derived via Hamilton's principle. The ordinary differential equations are formulated with the Galerkin discretization, which contain square and cubic nonlinear terms, parametric excitation terms and forcing excitation terms. The solutions of the governing equations verify the relationship between the steady-state nonlinear responses and the amplitudes and frequencies of parametric excitations. Finally, the Runge-Kutta method is utilized to obtain the periodic and chaotic motions from the governing equations.

The results of numerical simulation demonstrate the existence of the periodic and chaotic motions under the forcing excitations. The appropriate control technique of the forcing excitations contributes significantly to the influence on the responses of autonomous nonlinear systems. It is also found that there are same regular phenomena appearing in the different internal resonances of the CNT composite shell system.

Acknowledgement

The authors gratefully acknowledge the support of the National Natural Science Foundations of China (NNSFC) through grants Nos. 11202009 and 11572006, and the Funding Project for Academic Human Resources Development Institutions of Higher Learning under the Jurisdiction of Beijing Municipality (PHRIHLB).

References

1. K. T. Lau and D. Hui, The revolutionary creation of new advanced materials-carbon nanotube composites, *Composite: Part B* 33 (2002) 263-277.
2. S. Iijima, Helical microtubules of graphitic carbon, *nature(London)* 354 (1991) 56-58.
3. E. T. Thostenson, Z. Ren and T. W. Chou, Advances in the science and technology of carbon nanotubes and their composites: a review, *Composite Science Technology* 61 (2001) 1899-1912.
4. M. Griebel and J. Hamaekers, Molecular dynamics simulations of the elastic moduli of polymer-carbon nanotube composites, *Mechanical Engineering* 193 (2004) 1773-1788.
5. J. N. Coleman, U. Khan and Y. K. Gunko, Mechanical reinforcement of polymers using carbon nanotubes, *Advanced Materials* 18 (2006) 689-706.
6. Y. S. Song and J. R. Youn, Modeling of effective elastic properties for polymer based carbon nanotube composites, *Polymer* 47 (2006) 1741-1748.
7. P. Tan, L. Tong and X. Sun, Effective properties for plain weave composites through-thickness reinforced with carbon nanotube forests, *Composite Structure* 84 (2008) 1-10.
8. S. Xue and T. J. Pinnavai, Porous synthetic smectic clay for the reinforcement of epoxy polymers, *Microporous Mesoporous Mater* 107 (2008) 134-140.
9. J. K. Pandey, A. P. Kumar, M. Misra, A. K. Mohanty, L.T. Drzal, R. Palsingh, Recent advances in biodegradable nanocomposites, *Journal of Nanoscience and Nanotechnology* 5 (2005) 497-526.
10. K. Yang, X. Wang, Y. Wang, Progress in nanocomposite of biodegradable polymer, *Journal of Industrial and Engineering Chemistry* 13 (2007) 485-500.

11. P. Zhu, Z. X. Lei and K. M. Liew, Static and free vibration analyses of carbon nanotubes reinforced composite plates using finite element method with first order shear deformation plate theory, *Composite Structure* 94 (2012) 1450-1460.
12. H. S. Shen and Y. Xiang, Nonlinear vibration of nanotube-reinforced composite cylindrical shells in thermal environments, *Computer Methods in Applied Mechanics and Engineering* 213-216 (2012) 196-205.
13. S. Brischetto and E. Carrera, Classical and refined shell models for the analysis of nano-reinforced structures, *International Journal of Mechanical Science* 55 (2012) 104-117.
14. G. Bhardwaj, A. K. Upadhyay, R. Pandey and K. K. Shukla, Non-linear flexural and dynamic response of CNT reinforced laminated composite plates, *Composites Part B: Engineering* 45 (2013) 89-100.
15. R. Moradi-Dastjerdi, M. Foroutan and A. Poursghar, Dynamic analysis of functionally graded nanocomposite cylinders reinforced by carbon nanotube by a mesh-free method, *Material Design* 44 (2013) 256-266.
16. Z. X. Lei, L. W. Zhang, K. M. Liew and J. L. Yu, Dynamic stability analysis of carbon nanotube-reinforced functionally graded cylindrical panels using the element-free kpkp-Ritz method, *Composite Structure* 113 (2014) 328-338.
17. S. A. Fazelzadeh, S. Poursmaeeli and E. Ghavanloo, Aeroelastic characteristics of functionally graded carbon nanotube-reinforced composite plates under a supersonic flow, *Computer Methods in Applied Mechanics and Engineering* 285 (2015) 714-729.
18. P. Phung-Van, M. Abdel-Wahab, K. M. Liew, S.P.A. Bordas and H. Nguyen-Xuan, Isogeometric analysis of functionally graded carbon nanotube-reinforced composite plates using higher-order shear deformation theory, *Composite Structures* 123 (2015) 137-149.
19. Nguyen Dinh Duc, Homayoun Hadavinia, Pham Van Thu, Tran Quoc Quan, Vibration and nonlinear dynamic response of imperfect three-phase polymer nanocomposite panel resting on elastic foundations under hydrodynamic loads, *Composite Structures* 131 (2015) 229-237.
20. Gunasekaran Venugopal, Jipsa Chelora Veetil, Nivea Raghavan, Varu Singh, Ashwini Kumar and Azhagurajan Mukkannan, Nano-dynamic mechanical and thermal responses of single-walled carbon nanotubes reinforced polymer nanocomposite thinfilms, *Journal of Alloys and Compounds* 688 (2016) 454-459.
21. M. Amabili, Non-linear vibrations of doubly curved shallow shells, *International Journal of Non-Linear Mechanics* 40 (2005) 683-710.
22. V. A. Eremeyev and W. Pietraszkiewicz, Local symmetry group in the general theory of elastic shells, *Journal of Elasticity* 85 (2006) 125-152.
23. T. Park, S. Y. Lee, J. W. Seo and G. Z. Voyiadjis, Structural dynamic behavior of skew sandwich plates with laminated composite faces, *Composites: Part B* 39 (2008) 316-326.
24. J. Awrejcewicz, V. A. Krysko and A. V. Krysko, *Thermo-dynamics of plates and shells*, Springer, 2007.
25. M. Amabili, *Nonlinear vibrations and stability of shells and plates*, Cambridge University Press, 2008.
26. W. Zhang, X. Y. Guo and S. K. Lai, Research on periodic and chaotic oscillations of composite laminated plates with one-to-one internal resonance, *International Journal of Nonlinear Sciences and Numerical Simulation* 10 (2009) 1567-1583.
27. X. Y. Guo, W. Zhang and M. H. Yao, Nonlinear dynamics of angle-ply composite laminated thin plate with third-order shear deformation, Science in China Series E, *Technological Sciences* 53 (2010) 612-622.
28. K. A. Lazopoulos and A. K. Lazopoulos, Nonlinear strain gradient elastic thinshallow shells, *European Journal of Mechanics – A/Solids* 30 (2011) 286-292.

29. N. D. Duc and T. Q. Quan, Nonlinear response of imperfect eccentrically stiffened FGM cylindrical panels on elastic foundation subjected to mechanical loads, *European Journal of Mechanics A-Solids* 46 (2014) 60-71.
30. F. Alijani and M. Amabili, Non-linear vibrations of shells: A literature review from 2003 to 2013, *International Journal of Non-Linear Mechanics* 58 (2014) 233-257.
31. Y. Z. Liu, Y. X. Hao and W. Zhang, Nonlinear dynamics of initially imperfect functionally graded circular cylindrical shell under complex loads, *Journal of Sound and Vibration* 348 (2015) 294-328.
32. S. Tizzi, A free vibration analysis of toroidal composite shells in free space, *Journal of Sound and Vibration* 337 (2015) 116-134.
33. X.Y. Guo, W. Zhang, Nonlinear vibrations of a reinforced composite plate with carbon nanotubes, *Composite Structures* 135 (2016) 96-108.
34. D. L. Shi, X. Q. Feng, Y. Huang, K. C. Wang and H. Gao. The effect of nanotube waviness and agglomeration on the elastic property of carbon nanotubes-reinforced composites, *Journal of Engineering Materials and Technology* 126 (2004) 250-257.
35. T. Mori and K. Tanaka, Average stress in matrix and average elastic energy of materials with misfitting inclusions, *Acta Metall* 21 (1973) 571-574.